Research Open

Geology, Earth and Marine Sciences
Volume 6 Issue 4

Research Paper

The $CaCl_2$-to-Rutile Phase Transition in SnO_2 from High to Low Pressure in Nature

Rainer Thomas*

Im Waldwinkel 8, D-14662 Friesack, Germany

Corresponding author: Rainer Thomas, Im Waldwinkel 8, D-14662 Friesack, Germany

Received: May 27, 2024; **Accepted:** May 31, 2024; **Published:** June 06, 2024

Abstract

Raman studies on cassiterite from the Sauberg mine near Ehrenfriedersdorf showed that besides the tetragonal rutile-type phase in the root zone of a cassiterite vein, there is also present orthorhombic cassiterite with the $CaCl_2$ structure. According to Raman measurements, a maximal pressure of 18.9 GPa results. Such pressure implies the origin of that cassiterite from great depths, brought with supercritical fluids into the lower crustal level. The results show a reverse transition from high-pressure to low-pressure polymorphs of SnO_2 in nature.

Keywords: *Raman spectroscopy, Tetragonal and orthorhombic Cassiterite, $CaCl_2$-to-rutile transition, Supercritical fluids*

Introduction

The naturally occurring form of cassiterite is usually tetragonal, with the point group 4/m 2/m 2/m (point group number 128), and crystallizes as a rutile type phase. The paper by Thomas [1] described unusual cassiterite crystals from the tin deposit Ehrenfriedersdorf, Erzgebirge/Germany, as orthorhombic ones.

However, in the Balakrishnan et al. [2], only the bands at 446 (444 and 448 cm^{-1}) are present for the stable SnO_2 polymorphs. The data for the metastable phases are not given. All in all, the authors mentioned 20 relatively stable polymorphs. Seven stable polymorphs are tabulated. The band at 832 cm^{-1} is missing for all stable newly identified orthorhombic cassiterites. However, in the case of Ehrenfriedersdorf, at azimuthal rotation under the Raman microscope, some crystals show two unusual Raman bands at about 446 and 832 cm^{-1}, which are very strong at specific azimuthal positions and room temperature and room pressure. These authors (Balakrishnan et al., [2] have also stated that one polymorph can easily transformed into another by varying temperature or pressure. That must be true also for a combination of both variables. However, the transformation is sluggish enough to conserve precede phase states. In the case of the specific cassiterite from Ehrenfriedersdorf, we assume that the cassiterite came very fast from mantle deeps via supercritical fluids indicated by minerals like diamond, graphite, moissanite, OH-rich topaz, and the high-temperature feldspar kumdykolite [$NaAlSi_3O_8$] in the closer paragenesis [1]. Therefore, it is quite possible that at room temperature and pressure, "abnormal" cassiterite contains quenched remnants of high-temperature and high-pressure indications in the form of unusual Raman bands. This paper serves as a starting point for more systematic studies of cassiterite as a natural pressure sensor.

Sample Material

All sample material for this study came from a specimen, about 10 x 7 x 3 cm large, taken from the Prinzler counter vein in the Sauberg mine near Ehrenfriedersdorf by Puffe in 1936. The main minerals are quartz (~6 cm long), cassiterite (2 cm in diameter), and violet to green, sometimes pink fluorite (up to 1 cm in diameter). In the root zone, there are inclusions in different minerals (topaz, quartz, muscovite), which are generally tiny crystals of albite, kumdykolite, plagioclase, trilithionite, calcite, colorless high-temperature fluorite, OH-rich topaz, rynersonite, cassiterite, mangancolumbite, uraninite, monazite, xenotime, graphite, diamond, moissanite, and Ti-carbides [1]. Figures 1-3 show the studied cassiterite crystals, which are very different in appearance. In muscovite, there are smaller crystals beside the crystal shown in Figure 1, which are spherical or elliptical. The cassiterite crystal in Figure 2 is 500 µm thick as the tick section is. Figure 3 is a sizeable orthorhombic cassiterite crystal in spherical muscovite inclusion surrounded by dark tetragonal cassiterites. All cassiterites

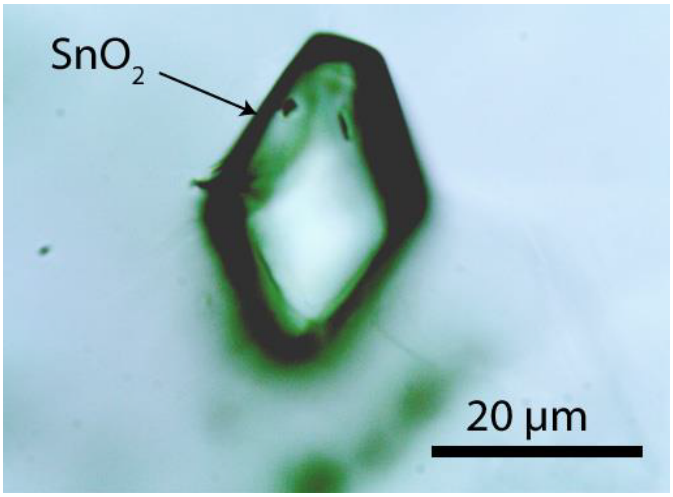

Figure 1: Cassiterite crystal I with rhombohedral cross-section in muscovite. The Raman bands of muscovite are entirely suppressed.

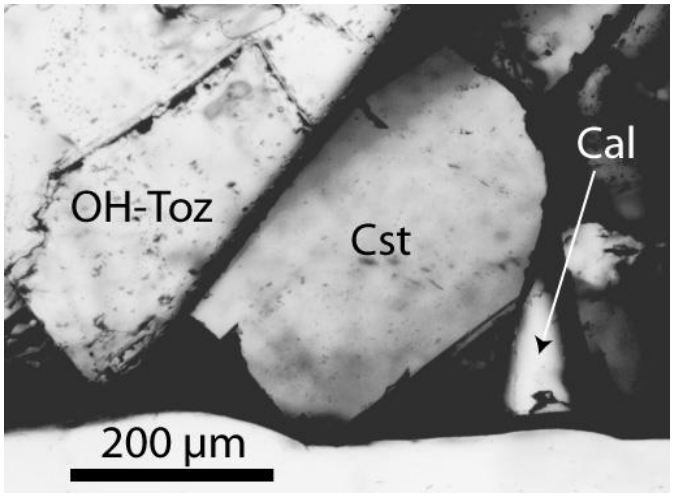

Figure 2: Cassiterite (Cst) crystall (crystal-II), about 250 x 390 µm large, beside tetragonal cassiterite (black), OH-rich topaz (OH-Toz) and calcite (Cal).

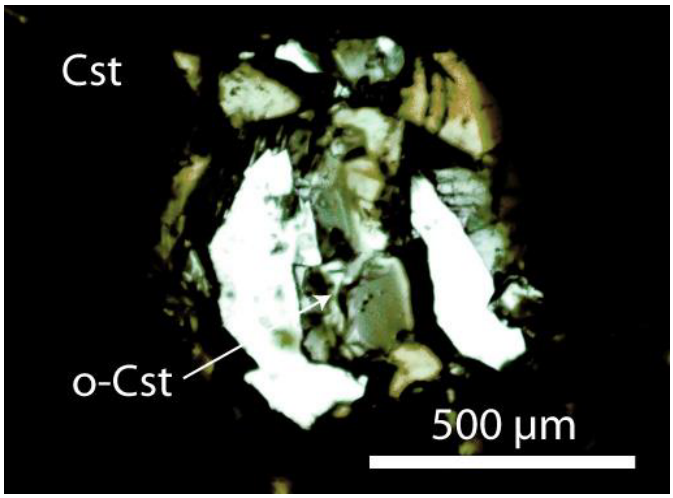

Figure 3: Large orthorhombic cassiterite crystal (o-Cst) in a muscovite inclusion (white) between normal tetragonal cassiterite (Cst). That is the sample cassiterite III.

with the untypical Raman bands at 445 and 832 cm^{-1} are inclusion-free, and the trace element concentration is low (about at the detection limit of the microprobe). Tiny crystals are colorless.

The differentiation between tetragonal and orthorhombic cassiterite is under the Raman microscope with a rotating stage simple. Rutile-type cassiterite shows at room temperature only one strong Raman band at about 633 cm^{-1} during azimuthal rotation under the polarized Raman light. Strong Raman bands at about 76, 448, 635, and 834 cm^{-1} are characteristically for orthorhombic cassiterite. The symmetry of the $CaCl_2$-type structure is orthorhombic and has the space group $P4_2/mnm$.

Microscopy and Raman Spectroscopy: Methodology

For the study of the cassiterite sample and the paragenetic minerals, we use the Zeiss JENALAB pol as well as the Raman spectrometer EnSpectr R532 combined with the Olympus BX43 microscope both for transmitted and reflected light and equipped with a rotating stage. For the identification of minerals and slight mineral inclusions, we used an Olympus long-distance LMPLFL100x objective lens. For the identification of different minerals, we used the RRUFF and the Hurai et al. [3] Raman mineral databases [3-4]. As references, we applied a water-clear diamond crystal from Brazil and a semiconductor-grade silicon single-crystal.

Results

In contrast to the typical tetragonal cassiterite of the Erzgebirge with the usual bands at 474, 633, and 775 cm^{-1} (both bands at 474 and 775 cm^{-1} are generally weak), the here-discussed cassiterite shows additional azimuthal-depending strong bands at 446, 832 cm^{-1}, beside the 633 cm^{-1} band [1]. In the compilation [2] of the Raman modes of stable SnO_2 polymorphs, only the orthorhombic cassiterite Pbcn (point group 2/m 2/m 2/m (number 60 in the room group list) contains a Raman active band at about 446 cm^{-1}. The 832 cm^{-1} band is completely missing in the list of polymorphs. Figure 4 shows a typical Raman spectrum of cassiterite crystal III. Conspicuous are the strong bands at 76, 448, 635, and 834 cm^{-1}.

According to the measurements of the Raman intensity of both bands (446 and 832 cm^{-1}), there is a good correlation shown in Figure 5. That means that both Raman bands belong together.

Because mineral inclusions in all the studied cassiterite crystals here are missing, the Raman bands are clearly components of the orthorhombic cassiterite, and both are strongly correlated. Also, the other crystals show a correlation between the two bands with near the same incline. That also will be clear from the following diagram (Figure 6). This figure shows the intensity ratio between the 633 and 832 cm^{-1} bands in dependence on the azimuth position. The figure (Figure 6) shows, in principle, the results for all three studied cassiterite crystals (I to III), which only show a peaks' position dependence on the crystal orientation (a synchronous shift of the maxima to right or left).

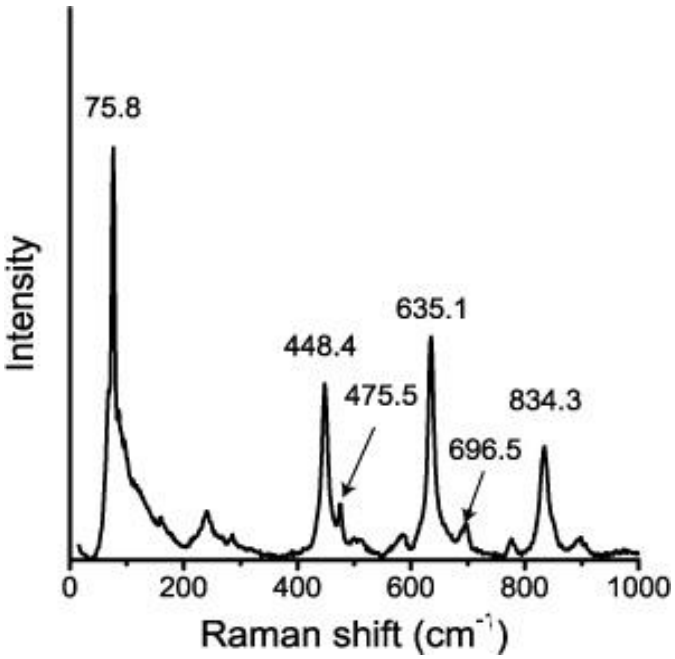

Figure 4: Raman spectrum (a choice of 46 spectra) of SnO_2 (sample III).

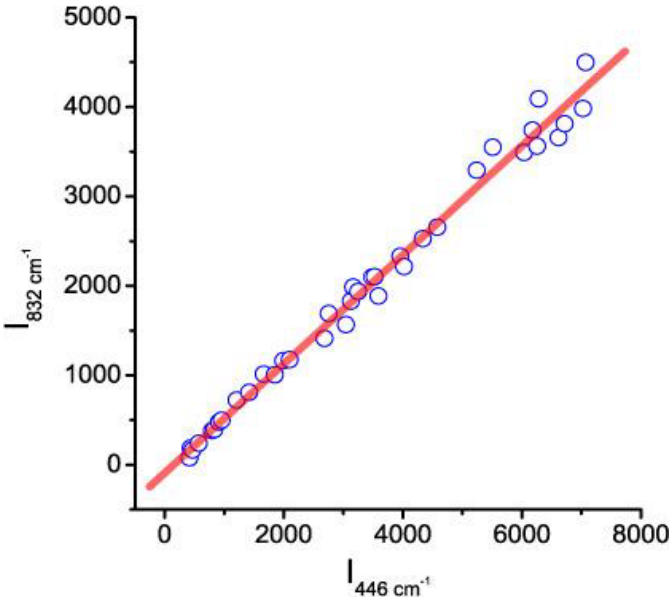

Figure 5: Correlation between the Raman intensity of the 446 and 832 cm^{-1} bands; I_{832} cm^{-1}=-89.829 + 0.609 * I_{446} cm^{-1}, r^2=0.989.

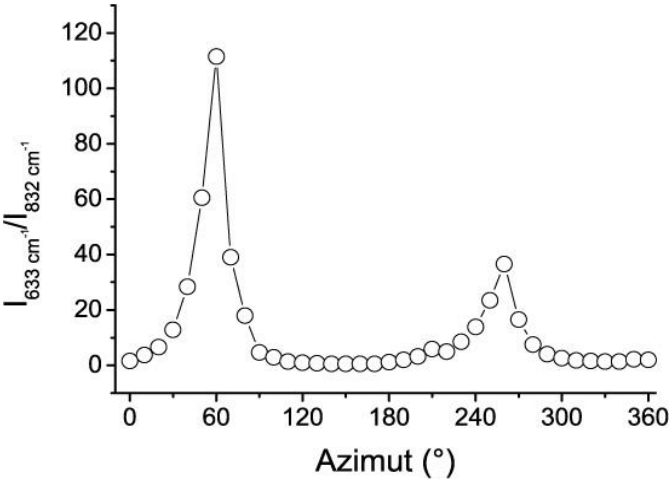

Figure 6: Intensity ratio between the 633 and the 832 cm^{-1} bands versus the azimuth position for crystal I. Similar figures resulted for the cassiterite crystals II and III.

Figure 7 shows the azimuthal Raman intensity distribution for the orthorhombic cassiterite main band at 633 cm^{-1}. The position of the points depends on the orientation of the studied sample. The points for the 446 and 832 Raman bands lie almost perpendicular to the 150° - 330° line. In the case of tetragonal cassiterite, the open red points would form a circle.

Interpretation

The Raman bands at 446, 633, and 832 cm^{-1} are strongly polarized, and the bands at 446 and 832 have a different symmetry - they are almost perpendicular to the 633 cm^{-1} band. The explanation is not simple. Have we, in this case, a different polymorph phase of SnO_2 not described in Balakrishnan et al., [2]? Or are the unusual Raman bands of SnO_2 frozen high-temperature and high-pressure remnants of the rutile-type, orthorhombic, or the $CaCl_2$ phase of cassiterite?. Note that in Figure 8, the points for the 832 cm^{-1} Raman band show a twisted form. From 38 measurements of the 832 cm^{-1} band on the cassiterite crystal-III, we obtain a mean of 833.9 ± 0.4 cm^{-1}. This value corresponds to Hellwig et al. [5] for the B_{2g} mode to a pressure of 10.5 GPa and falls into the rutile-type cassiterite. According to Girao [6], we can assume that the high-temperature and high-pressure cassiterite are well-crystallized (indicated by the intense and sharp Raman bands), are nano-particles in high concentrations, or contain larger domains. According to Girao [6] [Table 4, p.105], it results from the mean of 833.9 cm^{-1}, a pressure of about 15 GPa. This pressure marks the rutile- to $CaCl_2$-type transition. The rutile polymorph of SnO_2 underwent a phase transition to a $CaCl_2$ polymorph at 11.8 GPa under hydrostatic conditions [2]. Sometimes, we observe on the 833.9 band a shoulder at 849.7 ± 1.1 cm^{-1} (n = 10). Using Table 4 in Girao [6], it results in a pressure of 18.9 GPa and is, obviously, a high-pressure remnant of the $CaCl_2$-type cassiterite.

Generally, besides the 633 cm^{-1} prominent bands, small bands at 695.9 ± 2.1 cm^{-1} are present. After Figure 7 and Table 4 in Hellwig

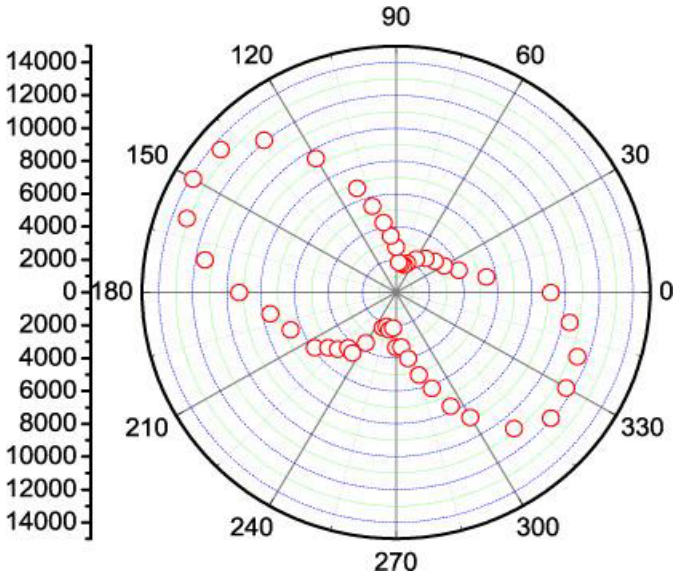

Figure 7: Cassiterite, crystal-III: Raman intensity distribution for the 633 cm^{-1} band in dependence on the azimuth position of the crystal. The numbers on the left are intensities.

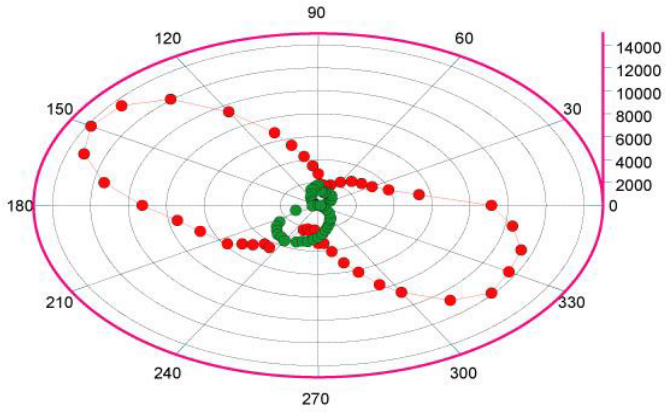

Figure 8: Cassiterite, crystal-III: Raman intensity distribution for the 633 cm^{-1} (red) and the 832 cm^{-1} (green) bands in dependence on the azimuth position of the crystal. The other orientation of the 832 cm^{-1} band is good to see. The measured intensities are the numbers on the right side of the diagram.

et al. [5], results for this A_{1g} mode band a pressure of 12.2 GPa and, according to Girao [6] [Figure 54 and Table 4], a pressure of 13.7 GPa. For the cassiterite crystal-III, we could also determine for the B_{1g} mode a mean of 76.1 ± 0.5 cm^{-1} (n = 46). The intensity of this Raman band is very high. Using Figure 8 in Hellwig et al. [5] results in a pressure of 10.8 GPa. By some uncertainties (strong asymmetry of this band) of the soft mode in the $CaCl_2$ phase [5], the 76.1 cm^{-1} band can also represent the $CaCl_2$-type phase. The symmetry is similar to the 446 and 832 cm^{-1} bands.

The band at 448.2 ± 0.4 cm^{-1} strongly correlated with the 833 cm^{-1} band (n = 38) (see Figure 5), resulting after Girao [6] only a pressure of 5.7 GPa. That means the freezing behavior for the different Raman bands of different SnO_2 polytypes is not regular.

Discussion

The exceptional Raman band at 832 cm^{-1}, shown at first by Thomas [1], can explained, according to Hellwig et al. [5] and Girao [6], as frozen remnants of high-pressure phases of rutile- and $CaCl_2$-type cassiterite structures.

Because together with the orthorhombic cassiterite at room temperature, there are also present high-pressure and high-temperature indicator minerals, like diamond, moissanite, Ti-carbides, and kumdykolite [1], the interpretation of the extreme Raman bands finds his explanation. That means that a part of the cassiterite of the Ehrenfriedersdorf Sauberg mine comes directly from the mantle regions. Schütze et al., [7] came after careful studies to the result that the Ehrenfriedersdorf granite presents the differentiation products of subducted altered ocean crust. The proof of high-pressure cassiterite (with signs up to 18.9 GPa) underlines this interpretation. After a couple of studies (for example, Thomas and Rericha, 2023) [8], the transport of high-pressure cassiterite (suspended as solid phases) happens via supercritical fluids from mantle regions to the crust. We have not considered the influence of the temperature on the band shift [9].

We found many deposits in the Erzgebirge (Germany) and the Slavkovsky les (Czech Republic), which prove the presence of orthorhombic cassiterites. More sophisticated studies on the natural cassiterite samples are necessary.

Acknowledgments

For the sample, we are grateful to Professor Ludwig Baumann (1929-2008) from the Mining Academy Freiberg. We thank Pierre Bouvier, Grenoble, France, and Jörg Acker, Cottbus, Germany, for the courtesy of critical references and for starting the discussion on the unusual cassiterite from Ehrenfriedersdorf.

References

1. Thomas R (2023) Unusual cassiterite mineralization, related to the Variscan tin-mineralization of the Ehrenfriedersdorf deposit, Germany. *Aspects in Mining & Mineral Science* 11 : 1233-1236.
2. Balakrishnan K, Veerapandy V, Fjellvåg H, Vajeeston P (2022) First-principles exploration into the physical and chemical properties of certain newly identified SnO_2 polymorphs. *ACS Omega* 7 : 10382-10393. [crossref]
3. Hurai V, Huraiova M, Slobodnik M, Thomas R (2015) Geofluids – Developments in Microthermometry, Spectroscopy, Thermodynamics, and Stable Isotopes. *Elsevier*, 489 pp.
4. Lafuente B, Downs RT, Yang H, Stone N (2015) The power of database: s RRUFF project. In: Armbruster T, Danisi RM (eds.). Highlights in mineralogical crystallography. *Berlin* 1-30.
5. Hellwig H, Goncharov AF, Gregoryanz E, Mao H, Hemley RJ (2003) Brillouin and Raman spectroscopy of the ferroelastic rutile-to $CaCl_2$ transition in SnO_2 at high pressure. *Physical Review* 67 : 174110-1174110-7
6. Girao HT (2018) Pressure-induced disorder in bulk and nanometric SnO_2. Material Chemistry, Theses, Université de Lyon, 139 pp.
7. Schütze H, Stiehl G, Wetzel K, Beuge P, Haberland R, et al. (1983) Isotopen-und elementgeochemische sowie radiogeochronologische Aussagen zur Herkunft des Ehrenfriedersdorfer Granits-Ableitung erster Modellvorstellungen. *ZFI-Mitteilungen* 76 : 232-254.
8. Thomas R, Rericha A (2023) The function of supercritical fluids for the solvus formation and enrichment of critical elements. *Geology, Earth and Marine Science* 5 : 1-4.
9. Diéguez A, Romano-Rodríguez A, Vilà A, Morante JR (2001) The complete Raman spectrum of nanometric SnO_2 particles. *Journal of Applied Physics* 90 s: 1550-1557.

Citation:

Thomas R (2023) The $CaCl_2$-to-Rutile Phase Transition in SnO_2 from High to Low Pressure in Nature. *Geol Earth Mar Sci* Volume 6(4): 1-4.